

HIGH-RESOLUTION IMAGING USING CAPON BEAMFORMERS FOR URBAN SENSING APPLICATIONS

Fauzia Ahmad and Moeness G. Amin

Radar Imaging Lab
Center for Advanced Communications
Villanova University
Villanova, PA 19085, USA.

E-mail : {fauzia.ahmad, moeness.amin}@villanova.edu

ABSTRACT

A wideband synthetic aperture radar system based on beamspace Capon beamforming is presented for urban sensing applications. Various effects of signal propagation through building materials are incorporated into the beamformer design. Proof of concept is provided using real data collected in a laboratory environment. Comparison between data-independent and scene-dependent beamformers is provided. The results show that the beamspace Capon beamformer outperforms the non-adaptive delay-and-sum beamformer.

Index Terms— Capon, High-Resolution, Through-the-wall, Beamforming.

1. INTRODUCTION

In the emerging area of urban sensing, there is a need for high-resolution imaging of stationary targets [1-2]. Delay-and-sum beamforming can provide high-resolution images at the expense of an enlarged array aperture. However, for urban sensing applications, use of a large array may not be feasible because of system constraints such as low cost, light weight, easy to deploy, and covert operation. Therefore, for a given aperture size, one must resort to high resolution adaptive schemes to overcome the limitations of Fourier based schemes. These high-resolution schemes not only provide high crossrange resolution but have good interference suppression capabilities due to their data-dependent nature.

One class of adaptive techniques is minimum variance beamforming derived from Capon's method [3]. Various versions of the Capon beamformer exist in literature and differ mainly in terms of the constraints applied and/or the assumptions made about the covariance matrix [4-6]. A Stepped-frequency Capon Beamformer, based on high-definition vector imaging (HDVI) technique [7], was recently presented for urban sensing applications [8]. In this scheme, the received data is first preprocessed by

applying frequency dependent phase delays so that the returns from the pixel being imaged are aligned at all array locations. The sample covariance matrix is then computed from snapshots that are generated by partitioning the preprocessed frequency-aperture data into overlapping contiguous subsets, each containing 80% of the frequency and 80% of the aperture. The optimum weights are determined by using the Capon method with an additional constraint on the norm of the weight vector to overcome the rank-deficiency of the autocovariance matrix. Since the entire process, comprising preprocessing, covariance matrix generation, and computation of optimum weights, is repeated for every pixel in the image, the computational load is tremendous. Although the improvements in image quality are evident, the high computational complexity prevents its exploitation for practical use.

In this paper, we present beamspace high-definition imaging (B-HDI) as an alternative for urban radar sensing applications. B-HDI provides imaging performance similar to that of HDVI but at a much reduced computational load [9]. In B-HDI, a plurality of image domain snapshots is first obtained by delay-and-sum beamforming of four subsets of measured data. This step is required only once during the entire process. For each pixel in the high-definition image, multiple beamspace snapshots are generated from the image domain snapshots, which are then used to estimate the autocovariance matrix. This beamspace covariance matrix is used by the quadratically constrained capon technique to compute the image pixel value.

2. QUADRATICALLY CONSTRAINED B-HDI CAPON BEAMFORMER

Consider an M -element line array. Each element can be used for both transmission and reception of electromagnetic radiation. Let the wall, through which the system is looking, have a thickness d_w and a dielectric constant ϵ . The wall lies in the (x,y) -plane, whereas the line array extends along the x -axis in the (x,z) -plane. The array can be placed against

the wall or at some standoff distance, z_{off} . Let the m -th transceiver, placed at location $\mathbf{x}_m = (x_m, z_{off})$ illuminate the scene with a stepped-frequency signal, consisting of K components. The complex amplitude of the returns, at each frequency, is measured at the same transceiver location only. For a single point target located at \mathbf{x}_p (at range R_p in the direction θ_p), the complex amplitude, y_{mk} , corresponding to the k -th frequency, ω_k , measured at the m -th transceiver is given by

$$y_{mk} = a(\mathbf{x}_p) \exp(-j\omega_k \tau_{mp}) \quad (1)$$

where $a(\mathbf{x}_p)$ is the complex reflectivity of the target at \mathbf{x}_p , and τ_{mp} is the two-way signal propagation delay, as shown in Fig. 1. This delay is given by

$$\tau_{mp} = \frac{2l_{1mp}}{c} + \frac{2l_{2mp}}{c/\sqrt{\varepsilon}} + \frac{2l_{3mp}}{c} \quad (2)$$

where c is the speed of light, and

$$l_{1mp} = \frac{-z_{off}}{\cos\theta_{mp}}, \quad l_{2mp} = \frac{d_w}{\cos\phi_{mp}}, \quad l_{3mp} = \frac{R_p \cos\theta_p - d_w}{\cos\theta_{mp}} \quad (3)$$

with

$$\phi_{mp} = \sin^{-1}\left(\frac{\sin\theta_{mp}}{\sqrt{\varepsilon}}\right) \quad (4)$$

$$\begin{aligned} & (R_p \sin\theta_p - (x_m - z_{off} \tan\theta_{mp}))^2 + (R_p \cos\theta_p)^2 \\ & = l_{2mp}^2 + l_{3mp}^2 - 2l_{3mp}l_{2mp} \cos(\pi + \phi_{mp} - \theta_{mp}) \end{aligned} \quad (5)$$

We note from (1) - (5) that the target location introduces a frequency-dependent phase delay of the transmitted signal, which varies with the position of the transceiver and is also a function of the wall parameters through which the system is looking. The data collection process is repeated at each transceiver location until all M locations have been exhausted.

2.1. Preprocessing

The region of interest is divided into Q pixels in range and angle. The pixel size is taken to be smaller than the resolution of the imaging system by a factor of L .

The $M \times K$ measured dataset is divided into four $M_1 \times K_1$ subsets that include the corner elements of the full data. Here, $M_1 = \lceil 0.8M \rceil$, $K_1 = \lceil 0.8K \rceil$. Each of the four subsets is then processed, using delay-and-sum beamforming, to generate corresponding image domain snapshots as follows. Each snapshot consists of Q pixels. For the q -th pixel, located at $\mathbf{x}_q = (R_q, \theta_q)$, phase delays, corresponding to each frequency and determined by the propagation path from the transceiver to \mathbf{x}_q , are applied to

the n -th subset data. The complex amplitude value, $\tilde{I}_n(\mathbf{x}_q)$, for the q -th pixel of the n -th image snapshot is then obtained by summing the delayed signals [2].

$$\tilde{I}_n(\mathbf{x}_q) = \sum_{k=1}^{K_1} \sum_{m=1}^{M_1} y_{mk,n} \exp(j\omega_k \tau_{mq,n}), \quad n = 1, 2, 3, 4 \quad (6)$$

where $\tau_{mq,n}$ is given by (2) with p replaced by q . We assume exact knowledge of the wall parameters, specifically, its thickness and dielectric constant. In this case, one can predict the exact path from the transceiver to the q -th pixel. This results in aligning the returns from a target at the q -th pixel location at all transceiver locations.

Once the four image domain snapshots have been computed, the high-resolution image, consisting of Q pixels, is generated as follows.

2.2. Beamspace Snapshots

For the q -th pixel of the high-resolution image, beamspace snapshots are formed from the image domain snapshots as follows. Consider the following 3×3 set of pixels of the n -th image domain snapshot,

$$\begin{bmatrix} \tilde{I}_n(R_q - L, \theta_q - L) & \tilde{I}_n(R_q - L, \theta_q) & \tilde{I}_n(R_q - L, \theta_q + L) \\ \tilde{I}_n(R_q, \theta_q - L) & \tilde{I}_n(R_q, \theta_q) & \tilde{I}_n(R_q, \theta_q + L) \\ \tilde{I}_n(R_q + L, \theta_q - L) & \tilde{I}_n(R_q + L, \theta_q) & \tilde{I}_n(R_q + L, \theta_q + L) \end{bmatrix} \quad (7)$$

Let \mathbf{b}_n be the 3×1 vector obtained by forming ‘‘beams’’, i.e. summing the pixels in (7) according to their distance from the q -th pixel.

$$\mathbf{b}_n = \begin{bmatrix} \tilde{I}_n(R_q, \theta_q) \\ \tilde{I}_n(R_q, \theta_q - L) + \tilde{I}_n(R_q, \theta_q + L) + \tilde{I}_n(R_q - L, \theta_q) + \tilde{I}_n(R_q + L, \theta_q) \\ \tilde{I}_n(R_q - L, \theta_q - L) + \tilde{I}_n(R_q - L, \theta_q + L) + \tilde{I}_n(R_q + L, \theta_q - L) + \tilde{I}_n(R_q + L, \theta_q + L) \end{bmatrix} \quad (8)$$

Note that the pixels adjacent to the q -th pixel have not been used to compute the beamspace snapshots. This is because the detail discernible in an image is dependent only on the range and angular resolutions of the imaging system, and the pixel grid is oversampled by a factor of L . The beamspace snapshots are formed so that the response of a point target, located at \mathbf{x}_q , will be $[1 \ 0 \ 0]\mathbf{b}_n, \forall n$.

2.3. Quadratically Constrained Capon Technique

The sample covariance matrix is given by

$$\mathbf{R} = \frac{1}{4} \sum_{n=1}^4 \mathbf{b}_n \mathbf{b}_n^H \quad (9)$$

Here, \mathbf{R} is a 3×3 matrix. Note that in HDVI, the covariance matrix has dimensions $M_1 K_1 \times M_1 K_1$.

The q -th pixel value (the RCS of the target) of the high-definition image is given by

$$I(\mathbf{x}_q) = \mathbf{w}_0^H \mathbf{R} \mathbf{w}_0 \quad (10)$$

where \mathbf{w}_0 is the solution of the quadratically constrained version of Capon's technique described by [7]

$$\min_{\mathbf{w}} \mathbf{w}^H \mathbf{R} \mathbf{w} \text{ such that } \mathbf{w}^H \mathbf{a} = 1 \text{ and } \mathbf{w}^H \mathbf{w} \leq \beta \quad (11)$$

Here, $\mathbf{a} = [1 \ 0 \ 0]^T$ is the steering vector (the point response to be preserved) and $\sqrt{\beta}$ is the length of the vector \mathbf{w}_0 .

The process described by (8)-(10) is repeated for each pixel location to generate the desired image.

3. EXPERIMENTAL RESULTS

A near-field wideband synthetic aperture through-the-wall radar was set up in the Radar Imaging Lab at Villanova University. The system block diagram is shown in Fig. 2. An Agilent network analyzer, Model ENA 5071B, was used to synthesize a 500 MHz signal, centered at 2.5 GHz, using 101 frequencies with a step size of 5 MHz. A horn antenna, with an operational bandwidth from 1.0 to 12.4 GHz, was used as the transceiver and mounted on Damaskos, Inc. Field Probe Scanner, model 7X7Y, to synthesize a 57-element line array with an interelement spacing of 2.2cm. A 12' x 8' segment of a 3" thick plywood wall was placed 0.8m in front of the antenna baseline. A conducting sphere of 12" diameter, located at 3.4m range and an angle of 2.2°, was used as the target, as shown in Fig. 3. For aperture synthesis, the set of 101 frequencies is transmitted from a single array element and the returns are received at the same array location only. This process is then repeated for the next array location until all of the 57 array locations are exhausted. The data measurement process for each array location consists of the following steps.

- 1) Background measurement. This is a measurement made of the received complex amplitude of all 101 monochromatic signals. The purpose of this experiment is to measure the clutter characteristics of the lab. The 12" sphere target is not present.
- 2) Target measurement. This is a complex amplitude measurement of the received signal across all 101 frequencies using the same exact setting as in the first experiment, but including the sphere.

The background data set is subtracted from the target data set for clutter reduction. This final data set, after clutter subtraction, was used for processing.

Figure 4 shows the image obtained using the delay-and-sum beamformer. Unit weights were applied to shape the beam. The image in Fig. 4 locates the target but exhibits high sidelobes and clutter. Figure 5 shows the image obtained using the beamspace Capon beamformer. For comparison, the image obtained using HDVI scheme of [7] is also provided in Fig. 6. For HDVI, 252 snapshots (46-by-

81 overlapping subsets of the 57-by-101 data matrix) were used to estimate the covariance matrix. For both HDVI and B-HDI, we used a value of 1.25 for β . We can clearly observe that the capon beamformers provide significant sidelobe and speckle reduction with resolution comparable to that of the delay-and-sum beamformer. In fact, the beamspace Capon provides better sidelobe suppression than HDVI.

4. CONCLUDING REMARKS

We have presented a computationally efficient adaptive stepped-frequency synthetic aperture beamformer for urban sensing applications based on the quadratically constrained beamspace Capon technique. Supporting results based on real data collected in laboratory environment are provided, depicting the superior performance of the new technique compared to the commonly applied delay-and-sum beamforming.

5. ACKNOWLEDGMENT

This work was supported by DARPA under contract no. MDA972-02-1-0022. The content of the information does not necessarily reflect the position or the policy of the Government, and no official endorsement should be inferred.

6. REFERENCES

- [1] V. Venkatasubramanian, H. Leung, "A novel chaos based high resolution imaging and its applications to through-the-wall imaging," *IEEE Signal Process. Lett.*, Vol. 12, No. 7, pp. 528-531, 2005.
- [2] G. Wang, M. G. Amin, "Imaging through unknown walls using different standoff distances," *IEEE Trans. Signal Process.*, Vol. 54, No. 10, pp. 4015-4025, 2006.
- [3] J. Capon, "High-resolution frequency wavenumber spectrum analysis," *Proc. IEEE*, Vol. 57, No. 8, pp. 1408-1411, 1969.
- [4] J. Li, P. Stoica, Z. Wang, "On robust capon beamforming and diagonal loading," *IEEE Trans. Signal Process.*, Vol. 53, No. 7, pp. 1702-1714, 2003.
- [5] B. D. Van Veen, "Minimum variance beamforming with soft response constraints," *IEEE Trans. Signal Process.*, Vol. 39, No. 9, pp. 1964-1972, 1993.
- [6] S. A. Vorobyov, A. B. Gershman, Z-Q. Luo, "Robust adaptive beamforming using worst-case performance optimization: A solution to the signal mismatch problem," *IEEE Trans. Signal Process.*, Vol. 51, No. 2, pp. 313-324, 2003.
- [7] G. R. Benitz, "High-Definition Vector Imaging," *Lincoln Lab Journal*, Vol. 10, No. 2, 1997.
- [8] F. Ahmad, M. G. Amin, S. A. Kassam, "A beamforming approach to stepped-frequency synthetic aperture through-the-wall radar imaging," *Proc. CAMSAP05*, Vol. 1, Dec. 2005.
- [9] G. R. Benitz, "High-Definition imaging apparatus and method", U.S. Patent No. 6,608,585, Aug. 2003.

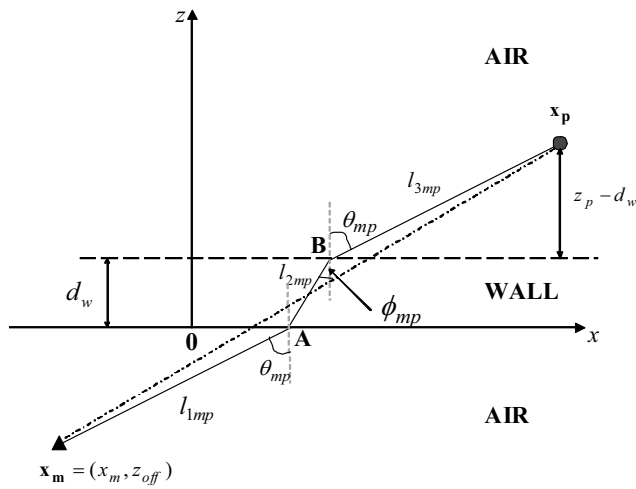


Fig. 1: Propagation through the wall.

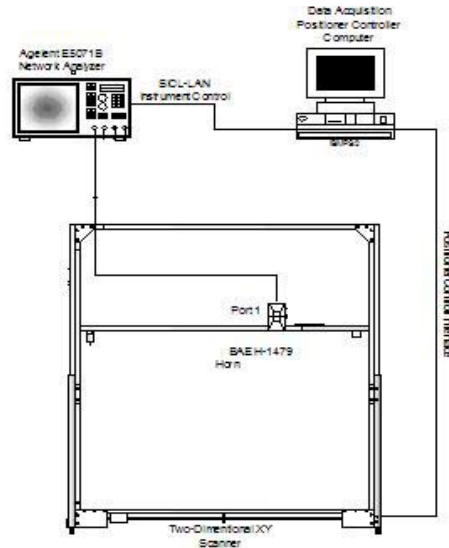


Fig. 2: System Block Diagram.

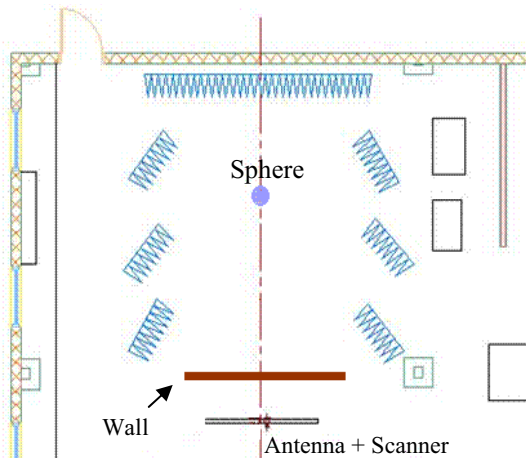


Fig. 3: Scene Layout.

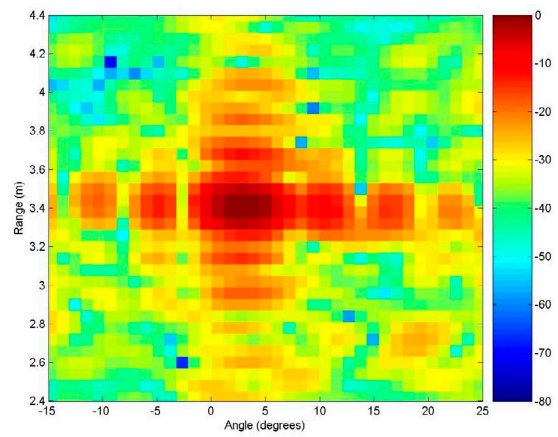


Fig. 4: Image obtained using delay-and-sum beamformer.

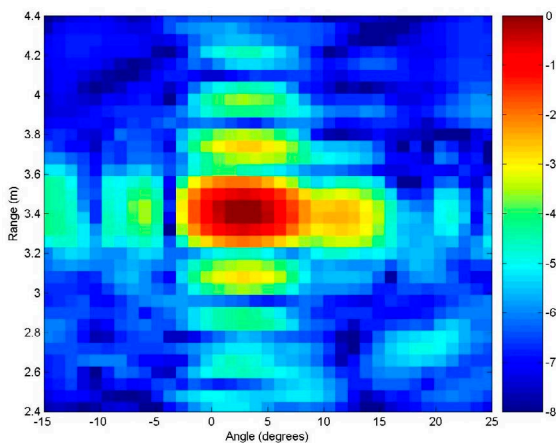


Fig. 5: Image obtained using B-HDI.

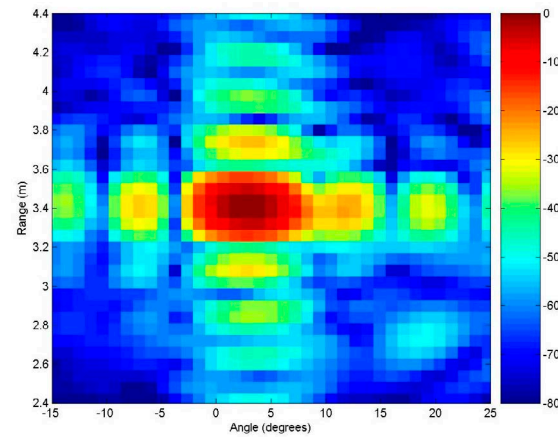


Fig. 6: Image obtained using HDVI.